ACADEMIC PRESS

Available online at www.sciencedirect.com

SCIENCE DIRECT®

Virology 316 (2003) 267–280

VIROLOGY

www.elsevier.com/locate/yviro

Release of canine parvovirus from endocytic vesicles

Sanna Suikkanen, Mia Antila, Anne Jaatinen, Maija Vihinen-Ranta, and Matti Vuento*

Department of Biological and Environmental Science, P.O. Box 35, FIN-40014 University of Jyväskylä, Finland

Received 10 June 2003; returned to author for revision 11 July 2003; accepted 4 August 2003

Abstract

Canine parvovirus (CPV) is a small nonenveloped virus with a single-stranded DNA genome. CPV enters cells by clathrin-mediated endocytosis and requires an acidic endosomal step for productive infection. Virion contains a potential nuclear localization signal as well as a phospholipase A_2 like domain in N-terminus of VP1. In this study we characterized the role of PLA_2 activity on CPV entry process. PLA_2 activity of CPV capsids was triggered in vitro by heat or acidic pH. PLA_2 inhibitors inhibited the viral proliferation suggesting that PLA_2 activity is needed for productive infection. The N-terminus of VP1 was exposed during the entry, suggesting that PLA_2 activity might have a role during endocytic entry. The presence of drugs modifying endocytosis (amiloride, bafilomycin A_1, brefeldin A, and monensin) caused viral proteins to remain in endosomal/lysosomal vesicles, even though the drugs were not able to inhibit the exposure of VP1 N-terminal end. These results indicate that the exposure of N-terminus of VP1 alone is not sufficient to allow CPV to proliferate. Some other pH-dependent changes are needed for productive infection. In addition to blocking endocytic entry, amiloride was able to block some postendocytic steps. The ability of CPV to permeabilize endosomal membranes was demonstrated by feeding cells with differently sized rhodamine-conjugated dextrans together with the CPV in the presence or in the absence of amiloride, bafilomycin A_1, brefeldin A, or monensin. Dextran with a molecular weight of 3000 was released from vesicles after 8 h of infection, while dextran with a molecular weight of 10,000 was mainly retained in vesicles. The results suggest that CPV infection does not cause disruption of endosomal vesicles. However, the permeability of endosomal membranes apparently changes during CPV infection, probably due to the PLA_2 activity of the virus. These results suggest that parvoviral PLA_2 activity is essential for productive infection and presumably utilized in membrane penetration process of the virus, but CPV also needs other pH-dependent changes or factors to be released to the cytoplasm from endocytic vesicles.

Keywords: Parvovirus; Entry; Endocytosis; Phospholipase A_2; Amiloride; Bafilomycin A_1; Brefeldin A; Monensin; Membrane permeabilization; Transferrin receptor

Introduction

The icosahedral, nonenveloped parvoviruses are among the smallest of the animal viruses. The atomic structure of canine parvovirus (CPV) capsid has been solved by X-ray crystallography (Tsao et al., 1991; Xie and Chapman, 1996). CPV particle has a diameter of about 26 nm (Agbandje et al., 1993). The capsid contains 60 protein subunits of which 90% are VP2 (67 kDa) and 10% VP1 (83 kDa). In full capsids containing DNA, some N-terminal ends of VP2 are exposed on the outside of the capsid and cleaved by host cell proteases to form VP3 (65 kDa) (Paradiso et al., 1982; Tattersall et al., 1977; Tullis et al., 1992; Weichert et al., 1998). The cleavage exposes the conserved glysine-rich sequence, which may be needed for interaction with cellular membranes (Tattersall and Cotmore, 1988). VP1 contains the complete amino acid sequence of VP2 in addition to a 143-residue unique N-teminal sequence that is buried within the capsid (Paradiso, 1981; Weichert et al., 1998). VP1 N-terminal end can be exposed by treatment at high temperature or with urea without complete disintegration of capsid (Cotmore et al., 1999; Vihinen-Ranta et al., 2002; Weichert et al., 1998). The canine parvovirus entry to the host cell starts by binding to transferrin receptors, followed by clathrin-mediated endocytosis and transport to the recycling endosomes (Parker et al., 2001; Suikkanen et al., 2002).

* Corresponding author. Fax: +358-14-260-2271.
E-mail address: vuento@bytl.jyu.fi (M. Vuento).

0042-6822/$ – see front matter © 2003 Elsevier Inc. All rights reserved.
doi:10.1016/j.virol.2003.08.031

Cytoplasmically microinjected antibodies to the transferrin receptor (TfR) cytoplasmic tail reduced CPV proliferation when injected into cells 4 h after inoculation, showing that many infecting capsids remain associated with the TfR in endocytic compartments for several hours after uptake (Parker et al., 2001). Before escape from endosomal vesicles to the cytosol, CPV was detected in lysosomes (Suikkanen et al., 2002). Antibodies to the CPV capsid injected into the cytoplasm also prevented CPV proliferation when injected at 6 h postinfection, indicating that CPV penetrates slowly out of the vesicles (Vihinen-Ranta et al., 2002).

Cytoplasmic microinjection of antibodies recognizing VP1 unique region inhibited the proliferation of CPV, indicating that VP1 became exposed before nuclear entry of CPV (Vihinen-Ranta et al., 2002). VP1 N-terminal end has an essential role during the parvovirus entry. Virions with their VP1 N-terminal unique sequence deleted were not able to cause productive infection (Tullis et al., 1993; Vihinen-Ranta et al., 2002). N-terminus of VP1 has been shown to contain a potential nuclear localization signal in CPV and in minute virus of mice (MVM) (Tullis et al., 1993; Vihinen-Ranta et al., 1997). A phospholipase A_2 (PLA_2)-like domain was found in the amino acid sequence of N-termini of VP1 of several parvoviruses (Zádori et al., 2001). The role of PLA_2 activity of the VP1 unique region of most parvoviruses has been demonstrated with inhibitors of PLA_2, and by mutations of the predicted active site, suggesting that the viral PLA_2 activity is needed at a step in the virus life cycle between perinuclear accumulation and early gene expression (Dorsch et al., 2002; Girod et al., 2002; Li et al., 2001; Zádori et al., 2001).

Several viruses that enter cells by clathrin-mediated endocytosis undergo structural changes needed for productive infection during endocytosis (Giranda et al., 1992; Kim et al., 1990). Structural changes may be induced by binding to the receptor with or without necessity for the virus to become exposed to low pH (with; Miyazawa et al., 2001; Seth et al., 1984a,b; Wickham et al., 1994; without: Greve et al., 1991; Hoover-Litty and Greve, 1993). The receptor-mediated endocytic uptake of picornaviruses and adenoviruses is followed by penetration through endosomal membrane (Marsh and Helenius, 1989). Poliovirus (a member of enteroviruses, a subfamily of picornaviruses) externalizes N-termini of VP1 and myristoylated VP4 in the presence of receptor both in vivo and in vitro, this leading to formation of an altered virus particle, the A particle (De Sena and Mandel, 1977; Gomez Yafal et al., 1993; Kaplan et al., 1990). The formed A-particle has been shown to interact with liposomes and to form ion channels in the membranes (Fricks and Hogle, 1990; Tosteson and Chow, 1997). Subgroup B adenoviruses (Ad7) have been shown to form aggregates in the endocytic compartment (Chardonnet and Dales, 1970; Dales and Chardonnet, 1973), and to cosediment and colocalize with lysosomal markers (Chardonnet and Dales, 1970; Miyazawa et al., 2001; Ogier et al., 1977). The optimal pH for lysis of endosomal membranes by Ad7 was shown to be 5.5, indicating that adenoviral disruption of endosomes might be optimal in low pH compartments such as late-endosomes or lysosomes (Miyazawa et al., 2001). In addition to low pH conditions, adenovirus-mediated endosomal membrane permeabilization requires the interaction of the virus proteins with the alphaV-integrin receptor (Seth et al., 1984a,b, 1985; Wickham et al., 1994). The mechanisms behind the membrane penetration process of CPV are not well characterized. However, endosomal escape of CPV particles did not allow release of coendocytosed alpha-sarcin to the cytoplasm, indicating that viral penetration through the endosomal membrane did not cause disruption of endosomes (Parker and Parrish, 2000).

The aim of the present study was to clarify the role of the VP1 N-terminal end and parvoviral phospholipase in CPV entry process. Intracellular pathway of CPV was studied using different inhibitors of endocytosis or phospholipase A_2 activity to gain further information about the viral escape from endosomal vesicles and intracellular conditions enabling successful infection. The results of this article indicated that parvoviral PLA_2 activity found from the N-terminal part of VP1 was triggered by treatments of acidic buffers or heating. That sequence was exposed also during the entry at 3–8 h p.i. in lysosomal vesicles, suggesting that acidic pH of lysosomal interior triggers the activation of viral PLA_2. This further suggests that PLA activity might be utilized in membrane penetration process. However, lysosomotropic drugs that inhibited viral proliferation did not inhibit exposure of the N-terminus of VP1. This indicates that PLA_2 activity was not alone sufficient to allow CPV to escape from endosomal vesicles. Some other pH-dependent factors must also be needed for CPV to be released from endocytic vesicles.

Results

Phospholipase A_2 activity of CPV capsids

CPV capsids heated at least at 55°C or incubated at acidic pH were tested for phospholipase A_2 activity. The results are shown in Figs. 1A and B. No activity was found in nontreated full capsids or in capsids incubated at temperatures below 50°C. When capsids were heated up to 55°C, they started to show PLA_2 activity. PLA_2 activity was also tested after pretreatment at pH 4.0–7.0 with or without neutralization step (Fig. 1A, without neutralization). CPV capsids that were treated with buffers with pH 4–6 showed PLA_2 activity. Similar results were obtained when capsids were neutralized after low pH treatment. The activity of heated CPV capsids was abolished in the presence of 5 mM EDTA and in the presence of quinacrine (QN) (2 mM; note

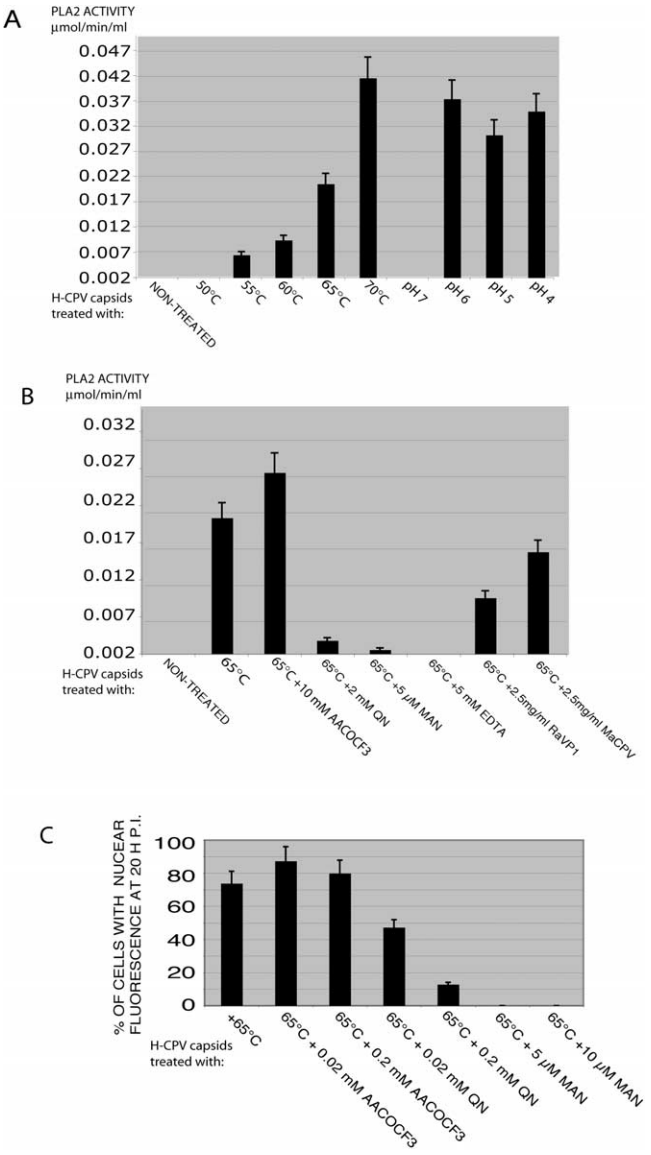

Fig. 1. PLA_2 activity of CPV capsid. (A) PLA_2 activity of heat-treated or low-pH-treated capsids. (B) PLA_2 activity of heat-treated capsids incubated (1 h) with PLA_2-inhibitors ($AACOCF_3$, QN, or MAN), EDTA, RaVP1, or MaVP2. (C) Effect of PLA_2 inhibitors on CPV proliferation. For technical details, please see Materials and methods.

that extra QN was removed by centrifugation before conducting the assay due to the strong yellow color of this reagent) or manoalide (MAN, 5 μM), inhibitors of secreted type PLA_2 (Fig. 1B). PLA_2 activity was also decreased by pretreating heated capsids with polyclonal rabbit antibody to CPV (RaVP1) antibody (2.5 mg/ml, Fig. 1B) compared to anticapsid antibody (mouse monoclonal antibody to CPV (MaCPV)) used at the same concentration. In contrast, inhibitor of cryptic phospholipase A_2 arachidonyl trifluoromethyl ketone ($AACOCF_3$) had no effect on PLA_2 activity. The effect of PLA_2 inhibitors on CPV infectivity was tested by inoculating cells with CPV capsids pretreated by heating (2 min, 65°C) and by incubation with phospholipase A_2 inhibitors for 2 h in RT (Fig. 1C). QN (0.2 mM) reduced CPV infectivity from 74 to 13% and MAN (5 or 10 μM) treated capsids were completely devoid of infectivity. Instead, no decrease of infectivity was found when full capsids were treated with of 0.2 mM $AACOCF_3$. Higher concentrations could not be tested because of the toxic effects exerted on cells by $AACOCF_3$.

Exposure of VP1 N-terminus during entry

To determine the time frame of exposure of the N-terminus of VP1 during entry, cells were inoculated with full capsids, fixed at 1 to 8 h p.i., and analyzed by double-labeling confocal immunofluorescence microscopy. For this purpose we used RaCPV as a primary antibody to stain capsids and MaVP1 to specifically detect VP1 proteins with exposed N-terminus. Results from such an experiment are shown in Fig. 2A. At 1 h post infection (p.i.) and later, RaCPV showed a predominantly perinuclear staining pattern (red color in Fig. 2A, 1 h p.i.). MaVP1 showed no staining at 1 h p.i. (lack of green color and lack of yellow color in merge-field Fig. 2A, 1 h p.i.). At 2–8 h p.i. MaVP1 antibody showed staining (green color in Fig. 2A) that was perinuclear and merged with the red staining given by RaCPV antibody. At 8 h p.i. the two perinuclear staining patterns merged extensively, indicating that many virus capsids showed exposed N-terminal ends of VP1 (Fig. 2A).

The antibiotic drug bafilomycin A_1 (BFLA) has been shown to inhibit proliferation of CPV and in the presence of BFLA capsids were detected in endosomal vesicles (Parker and Parrish, 2000). As BFLA and related drugs could be expected to modify the intravesicular conditions by elevating the luminal pH, it was of interest to test whether they could prevent the N-terminus of VP1 to become exposed. The above experiment was repeated (Fig. 2B) in the presence of 0.4 mM amiloride (AMI), 500 nM BFLA, 20 nM brefeldin A (BFA), or 500 nM monensin (MON). The exposure of the N-terminal end of VP1 was detected as colocalization (Fig. 2B, yellow color in merge field) between MaVP1 and RaCPV, despite the presence of any of these drugs. All four drugs were able to significantly inhibit the proliferation of CPV when they were added 2 h p.i. or earlier (Fig. 3A). When added 0 h p.i., the drugs caused a complete inhibition of proliferation. AMI and BFA still caused a significant inhibition when they were added at 8 h p.i., at which time the two other drugs no longer inhibited viral proliferation. In fact, AMI was able to inhibit the proliferation also when it was added as late as 16 h p.i. (Fig. 3A). A double-labeling immunofluorescence analysis of cells at 20 h p.i in the presence of 0.4 mM AMI, 500 nM BFLA, or 500 nM MON showed that CPV, when detected with RaCPV as the primary antibody, was present mostly in perinuclear vesicles that costained extensively with antibodies to lysosomal membrane protein-2 (LAMP-2) used as a marker for late endosomes and lysosomes, but not with early endosomal marker (EEA1) (Figs. 3B and C). In the

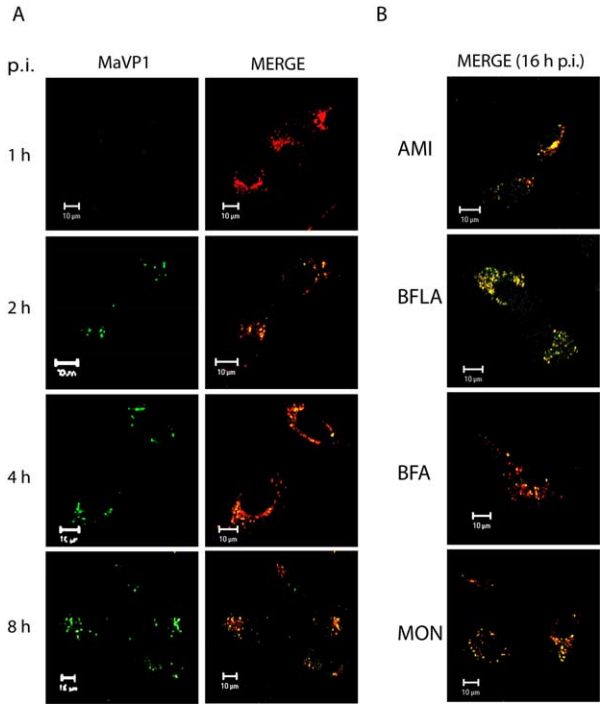

Fig. 2. Double-labeling confocal immunofluorescence microscopy of CPV endocytosed by NLFK cells. Exposure of N-terminus of VP1. Endocytosed CPV was chased for the time indicated. (A) Left column, staining with MaVP1 antibody (specific for the unique part of VP1 N-terminus, green color) as the primary antibody. Right column, merged images with capsids labeled with RaCPV (specific for CPV capsids, red color) and MaVP1 antibody (green). Colocalization, yellow color. (B) CPV chased for 16 h in the presence of AMI (0.4 mM), BFLA (500 nM), BFA (20 nM) or MON (500 nM). Merged images with capsids labeled with RaCPV (specific for CPV capsids, red color) and MaVP1 antibody (green). Colocalization, yellow color. Bars 10 μm.

presence of 20 nM BFA CPV was found to colocalize to a certain extent with both antibodies to EEA1 and with LAMP-2. Some confocal images (not shown) suggested that CPV forms aggregates to the vesicular membrane. This seemed to take place even in the presence of the above drugs. The presence of aggregates was confirmed by immunoelectron microscopy (Fig. 4). In the presence of BFLA and MON, gold labels indicating the presence of capsids were found as clusters from the membranes of late-endosomal and lysosomal resembling vesicles. In the presence of AMI the gold label was again mainly found at the lysosomal membrane, in addition to few cytoplasmic aggregates of the label. The label on the cytoplasmic face was bound to CPV capsids possibly caught in the process of penetrating through the membrane. In controls with no drugs added, some proportion of the label was found to be in the cytoplasm, while some label remained in contact with the lysosomal membrane. The results support the view that AMI, BFLA, MON, and BFA inhibit the escape of CPV from lysosomes. However, they did not prevent binding of CPV to the lysosomal membrane.

Microinjections of CPV and infections with heat-treated capsids in the presence of bafilomycin A_1, monensin, brefeldin A, and amiloride

To determine whether inhibition of CPV proliferation by the above drugs could be due to some postendocytic step(s) blocked by these drugs, low concentrations of nontreated CPV was microinjected to cytoplasm of drug-treated NLFK cells and localization of the capsids or appearance of NS1-protein was studied with immunofluorescence microscopy (not shown). Nuclear NS1 proteins and viruses (not shown) were now observed in the presence of 500 nM BFLA, 500 nM MON, and 20 nM BFA, as well as in controls (no drugs added), but not in the presence of 0.4 mM AMI (not shown). The results confirm that the inhibitory action of BFLA,

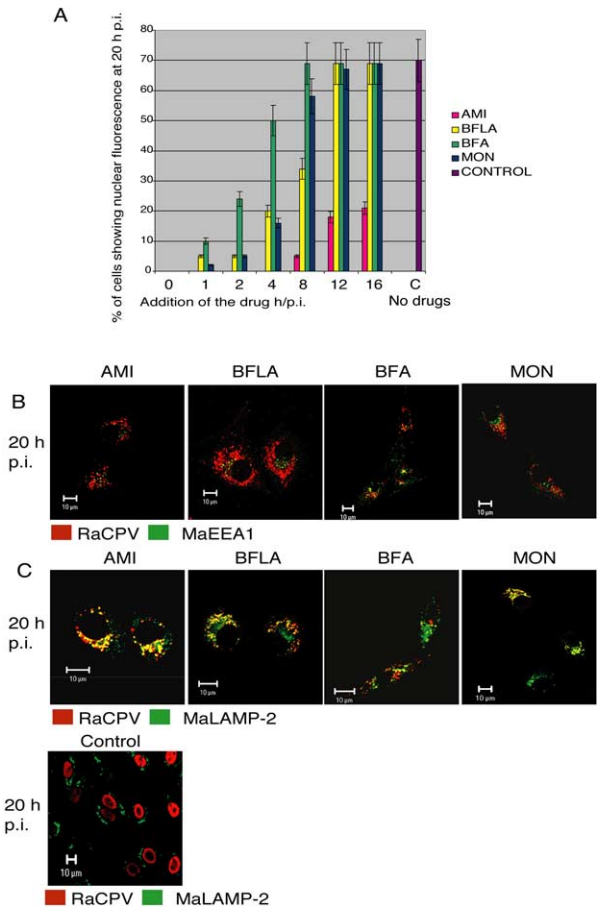

Fig. 3. Proliferation and endocytosis of CPV in the presence of lysosomotropic drugs. (A) Endocytosed CPV was chased for 20 h in the presence of 500 nM bafilomycin A_1, 500 nM monensin, 20 nM brefeldin A, or 0.4 mM amiloride. Control, no drugs. Infected cells were labeled with antibody to CPV capsids. Percentage of cells showing CPV proliferation (nuclear fluorescence) at 20 h p.i. was determined. The drugs were added at the indicated time points. (B) Labeling with antibody to CPV capsid (green color) and antibody to EEA1 (red color); colocalization, yellow color. Bars 10μm. (C) Labeling with antibody to CPV capsid (green color) and antibody to LAMP-2 (red color); colocalization, yellow color. Bars 10 μm. Control (no drugs) was also labeled with antibody to CPV capsid (red color) and antibody to LAMP-2 (green color).

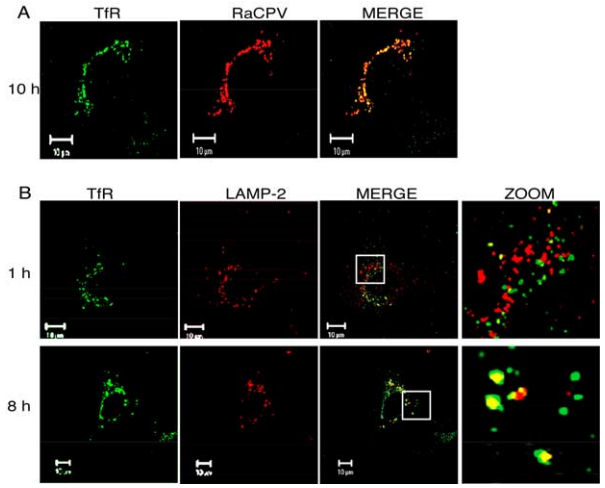

Fig. 6. Double-labeling confocal immunofluorescence microscopy. (A) Colocalization of endocytosed CPV with transferrin receptors. Endocytosed CPV was chased for the time indicated. Staining with RaCPV antibody (red color) as the primary antibody and with two different monoclonal antitransferrin receptor antibodies (green color). Colocalization, yellow color. (B) Intracellular distribution of transferrin receptors and LAMP-2. NLFK cells infected with CPV were fixed at 1 or 8 h p.i. as indicated and immunolabeled with two different monoclonal antitransferrin receptor antibodies (green color) and with Texas red conjugated LAMP-2. Colocalization, yellow color. Areas marked with white squares are shown in high magnification in the rightmost column (ZOOM).

MON, and BFA (Fig. 3) was due to effects they exerted on the endocytic route. In contrast, it appears that AMI inhibited some steps in the entry route or proliferation of CPV that occurred after release of CPV from the endosomal/lysosomal vesicles.

To further elucidate the importance of VP1 N-terminus in release of the virus from vesicles, cells were infected with heat-treated (65°C) capsids showing PLA_2 activity. Infectivity was determined by immunofluorescence labeling of NS1 or CPV capsid proteins after which percentage of cells showing nuclear fluorescence was counted from 300 cells/sample. Such capsids retained infectivity (Fig. 5), but the infection was strongly inhibited by added drugs. Since the drugs were able to inhibit proliferation of heat-treated CPV having exposed N-terminus of VP1, it appears that exposure of VP1 N-terminus was not the target of the inhibitory effect of these drugs.

Colocalization of CPV with TfR during entry

The interaction of CPV with TfR was studied with LSM by double labeling of infected cells fixed different time points postinfection with two different monoclonal antibodies to TfRs and with polyclonal antibody to CPV capsids. CPV was found to colocalize with TfR for at least 10 h (Fig. 6A). Furthermore, TfR was found to colocalize in infected cells with LAMP-2 at 8 h p.i. (Fig. 6B). At 1 h p.i. as well as in noninfected cells only some colocalization was found between TfRs and lysosomal vesicles.

CPV-induced release of dextran particles from lysosomal structures

The electron micrographs of Fig. 4 may show CPV in the process of penetrating the lysosomal membrane, but the present resolution does not allow conclusions of mechanism of penetration. To study further the mechanism of parvoviral escape from endosomal vesicles, we coendocytosed CPV with rhodamin-conjugated dextrans and chased for 2–20 h. In noninfected control cells, the rhodamine label of the M_r 3000 dextran was found in vesicular-like structures over the entire cytoplasmic cross section (Fig. 7A). A double-labeling fluorescence/immunofluorescence analysis is shown in Fig. 7B (dextran red, MaCPV-labeled CPV green). According to fluorescence microscopy analysis, coendocytosed dextrans did not disturb CPV entry or proliferation. In cells infected with CPV, dextran molecular size

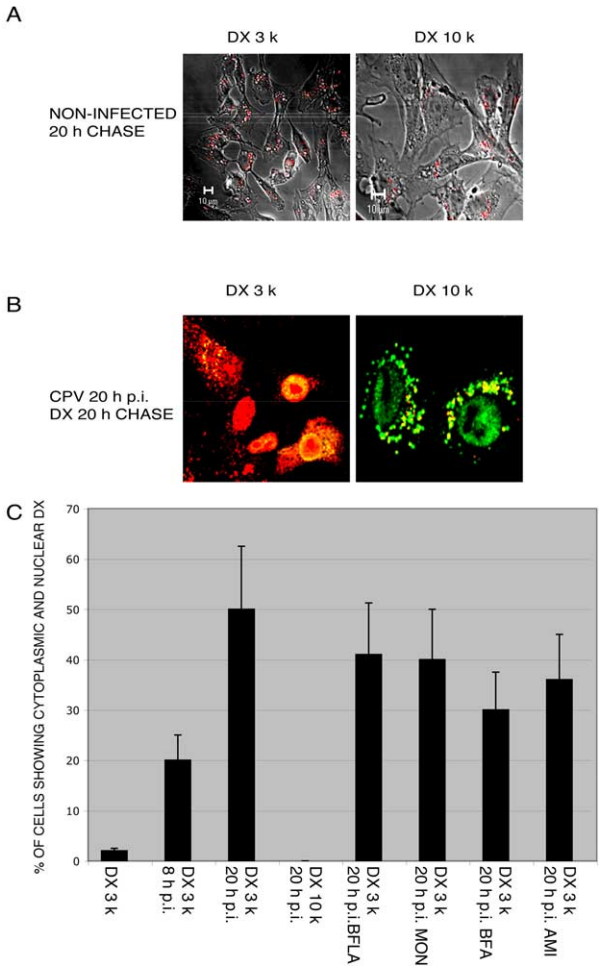

Fig. 7. Release of dextran coendocytosed with CPV. (A) Dextrans endocytosed by noninfected cells and chased for 20 h (B) Double-labeling confocal immunofluorescence staining. CPV and rhodamine-labeled dextrans were coendocytosed by NLFK cells and chased for 20 h. On the left, dextran with an M_r of 3000 was used; on the right dextran had a M_r of 10,000. Red color, rhodamine; green color, CPV; yellow color, colocalization. (C) Quantitative analysis of cells showing cytoplasmic and nuclear dextran.

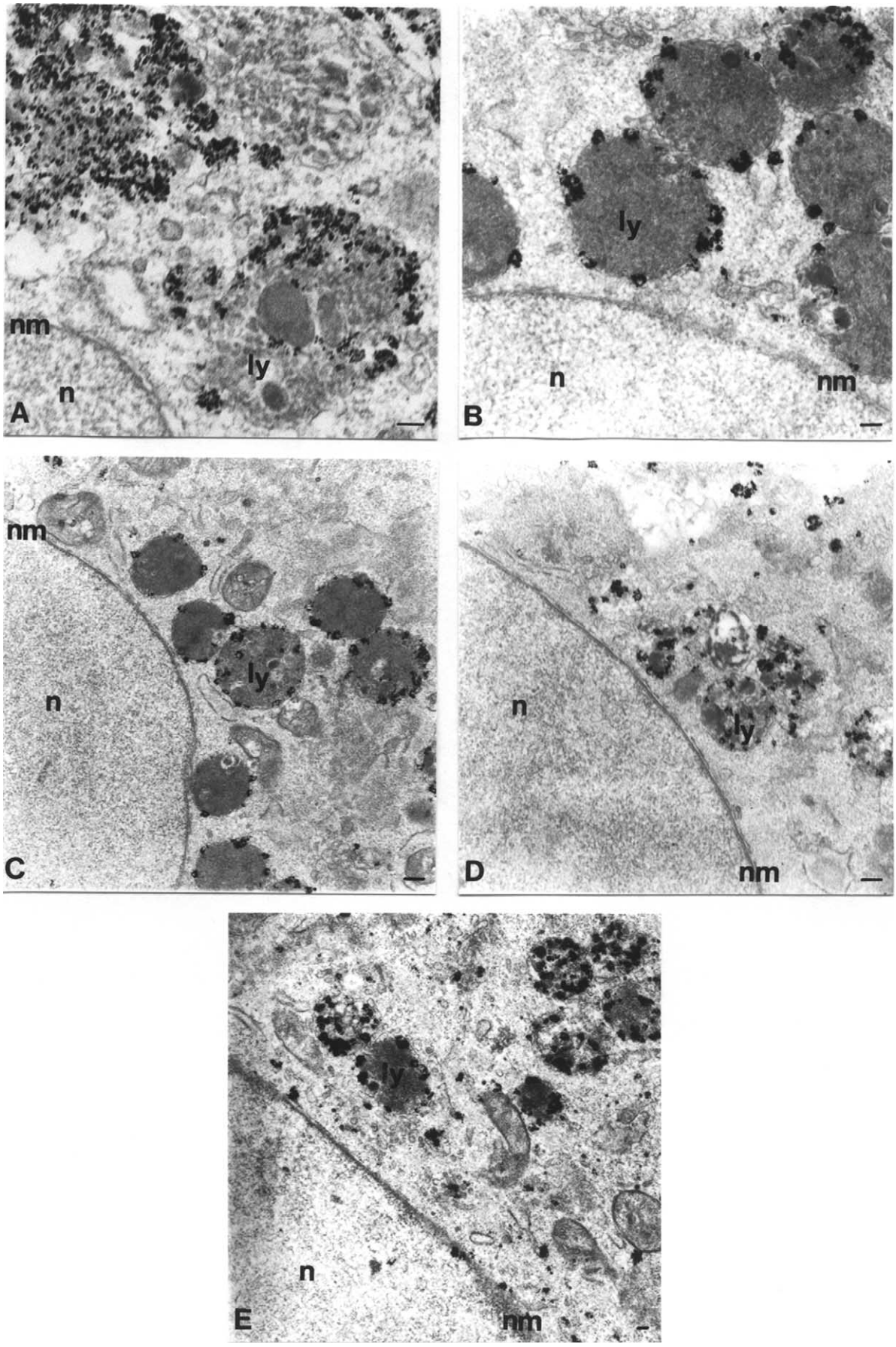

Fig. 4. Immunoelectron microscopy of CPV endocytosed by NLFK cells in the presence of lysosomotropic drugs. Nanogold labeling with silver enhancement. Endocytosed CPV was chased for 20 h in the presence of (A) AMI (0.4 mM), (B) BFLA (500 nM), (C) BFA (20 nM), or (D) MON (500 nM). (E) Control: no drugs present. Nucleus (n), nuclear membrane (nm), lysosome (ly) are marked in the figure. Bars, 100 nm.

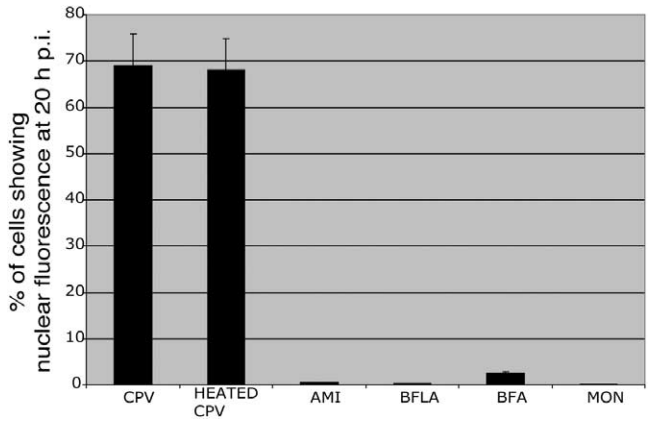

Fig. 5. Infectivity of heat-treated CPV in the presence of lysosomotropic drugs. Cells were inoculated with heat-treated (65°C) CPV in the presence of 500 nM BFLA, 500 nM MON, 20 nM BFA, or 0.4 mM AMI and fixed at 20 h p.i. Control: no drugs present. Cells were immunolabeled with MaCPV. Percentage of infected cells with fluorescent nuclei was counted ($n = 300$).

of 3000 was found in cytoplasm and in nucleus (red). Release of dextran was detected also in cells, where CPV was not yet detected in the nucleus. In contrast, the M_r 10,000 was retained exclusively in perinuclear vesicles both in noninfected control cells (right frame in Fig. 7A) and in infected cells (right frame in Fig. 7B). To quantify these results, the percentage of cells showing released (cytoplasmical/nuclear) dextran was counted in the presence or absence of lysosomotropic drugs (Fig. 7C). In noninfected control cells only few cells (1–3%) showed cytoplasmic or nuclear dextran and no release of M_r 10,000 dextran was detected in control cells or in infected cells even after 20 h of infection. In contrast, M_r 3000 dextran was released to cytoplasm in infected cells at 8 h p.i. and more cells showing cytoplasmic and nuclear dextran were detected at 20 h p.i. In infected cells treated with 0.4 mM AMI, 500 nM BFLA, 20 nM BFA, or 500 nM MON the M_r 3000 dextran was released to the cytoplasm, suggesting that these drugs were not able to inhibit viral endosomal membrane permeabilization. In noninfected cells AMI, BFLA, BFA, or MON caused no increase in the amount of cells showing released dextran (not shown). The results suggest that CPV modified late-endosomal/lysosomal membrane so that small-sized dextrans (M_r 3000) could leak out, while larger dextrans (M_r 10 000) were mainly retained in the lysosomes.

CPV capsid interaction with lipids

Because membrane lipids are not randomly distributed along endocytic pathways and their organelles (Simonsen et al., 2001), it was of interest to study the lipid-binding properties of CPV. Clathrin-coated vesicles (CCVs) are enriched in phosphatidylinositol 4- and 5-phosphates (PtdIns $(4,5)P_2$) (Simonsen et al., 2001). Phosphatidylinositol-3-phosphates are concentrated to early endosomal membranes, while lysophosphatidic acid and phosphatidylinositol-3,5-bisphosphate (PtdIns $(3,5)P_2$) are typical lipids for late endosomes (Kobayashi et al., 1998, 2002; Shisheva et al., 2001). In contrast, sphingolipids and sulfatide are abundant in recycling endosomes (Gagescu et al., 2000; Hölttä-Vuori et al., 2002). In this study interactions of CPV capsids with lipids were studied with arrays of phosphatidylinositols and sphingolipids (Molecular Probes). CPV was found to bind to phosphatidylinositol-4-phosphate (PtdIns(4)P), phosphatidylinositol-5-phosphate (PtdIns(5)P), and phosphatidylinositol-3,5-bisphosphate (PtdIns$(3,5)P_2$). Some binding was detected also with PtdIns(3)P, PtdIns(3,4)P, PtdIns(4,5)P, PtdIns(3,4,5)P, and with phosphatidyl serine. These results suggest that CPV capsids are able to bind to several membrane lipids found in the membranes of many different endocytic organelles, including at least clathrin-coated vesicles, early endosomes recycling endosomes, and late endosomes. Five mM of EDTA abolished CPV's ability to bind to these lipids. Heated capsids and VP1 antibody-treated capsids had equal ability to bind to lipids as untreated capsids, suggesting that VP1 N-terminus or its PLA_2 domain is not responsible for lipid binding activity. Furthermore, CPV bound to sulfatide. Binding to sulfatide was not inhibited by 5 mM EDTA.

Discussion

An interesting feature of the parvovirus capsid is the capability of N-terminal unique sequence of VP1 to undergo conformational changes. VP1 N-terminus is not accessible in intact capsids but it is externalized in specific conditions such as by heating or urea treatment, without complete capsid disintegration (Cotmore et al., 1999; Vihinen-Ranta et al., 2000; Weichert et al., 1998). Recently sequence analysis revealed the presence of domains resembling $sPLA_2$ active sites in N-terminus of VP1 of diverse parvoviruses including CPV (Zádori et al., 2001). In the present study we show that PLA_2 activity of CPV capsids was triggered by heating the capsids (Fig. 1A). PLA_2 activity was not found in nontreated capsids or capsids heated at 50°C. Instead, capsids heated at 55°C or higher temperature showed PLA_2 activity. As N-terminus of VP1 has been shown to be exposed by heating CPV capsids to 55°C by Western blots (Vihinen-Ranta et al., 2002), it appears that exposure of the N-terminus and activation of PLA_2 are interconnected. It follows that the PLA_2 activity could be used as a measure of exposure of the N-terminal unique sequence. In addition, capsids treated with low pH (4–6) buffer had PLA_2 activity (Fig. 1B), suggesting that the low pH of early endosomes or recycling endosomes is enough to trigger PLA_2 activity of CPV capsids during the endocytic entry. Our results supported the earlier data indicating that PLA_2-like domain of N-terminal end of VP1 sequence acts as secreted-type PLA_2 ($sPLA_2$) in parvoviral capsids as the activity of the capsids was inhibited by antibodies against N-terminal end of VP1, inhibitors of $sPLA_2$ QN and MAN,

or by 5 mM EDTA (Fig. 1B). Because this activity was triggered by acidic pH that is found in endosomes, it was of interest to test whether inhibitors of PLA_2 could affect endocytic entry of CPV. To study the role of PLA_2 activity, we treated capsids showing exposed VP1 N-terminals with PLA_2 inhibitors and used them for infections. MAN and QN, which were able to inhibit viral $sPLA_2$ activity, were also able to reduce the amount of cells with productive infection (Fig. 1C), indicating that viral PLA_2 is essential for the productive infection. This result is in line with earlier results, where PLA_2 activity of the VP1 unique region of porcine parvovirus (PPV), human parvovirus B19, and adenoassociated virus type 2 (AAV2) has been shown by PLA_2 inhibitor studies, and by mutations of the predicted active site, proposing that the parvoviral PLA_2 activity is needed during some step(s) of viral life cycle between perinuclear accumulation and early gene expression (Dorsch et al., 2002; Girod et al., 2002; Li et al., 2001; Zádori et al., 2001). We show here, by using antibodies specific to the N-terminal part of VP1 together with anticapsid antibody, that the VP1 N-terminal sequence became exposed during the endocytic entry of CPV (Fig. 2A) at the time when CPV had reached lysosomes. The lysosomal location of CPV at this time point was also reported in earlier work (Suikkanen et al., 2002). The results suggest that PLA_2 activity can be utilized for the membrane penetration by CPV when CPV escapes from lysosomes. Our earlier results as well as present results suggested that lysosomal vesicles are the probable site of escape for CPV to the cytoplasm (Suikkanen et al., 2002).

Acidification is known to be an important factor for successful parvovirus entry since drugs that change endosomal pH are able to block the infections (Bartlett et al., 2000; Basak and Turner, 1992; Douar et al., 2001; Parker et al., 2001; Ros et al., 2002; Vihinen-Ranta et al., 1998). In the present study further information was collected about the conditions that are needed for successful entry process using four different drugs (AMI, BFA, BFLA, and MON) modifying endocytosis. AMI is an inhibitor of Na^+/H^+ exchangers, which have been found at plasma membrane as a part of the machinery that maintains the neutral pH of cytosol (Noel and Pouyssegur, 1995; Yun et al., 1995). BFA is thought to interfere with trafficking between early and late endosomes and to have multiple effects on morphology of endocytic organelles (Lippincott-Schwartz et al., 1991). BFLA has been shown to cause inhibition of receptor–ligand dissociation (Harada et al., 1997), inhibit endosomal carrier vesicle formation (Clague et al., 1994) and late endosome-lysosome fusion (Van Weert et al., 1995), as well as cause fragmentation of early endosomes (D'arrigo et al., 1997). MON, Na^+/H^+ ionophore is known to raise pH of all intracellular acidic compartments by exchanging of protons for monovalent cations (reviewed in Pressman, 1976) and thus, causing similar intracellular effects to those of BFLA. Moreover, it has been shown that transferrin intake remains intact in the presence of MON and BFLA (Johnson et al., 1993; Stein and Sussman, 1986). In the present work, BFLA and MON were able to block CPV infection (Fig. 3), being in line with the earlier results indicating that parvoviral entry is pH-dependent. In addition, we found BFA and AMI to be potent inhibitors of CPV proliferation (Fig. 3). BFA has been also found to inhibit MVM proliferation (Ros et al., 2002). In the presence of BFA some capsids showed colocalization with early endosomal as well as with lysosomal markers, probably because the membranes of endocytic machinery are somewhat mixed or the trafficking from early endosomes is slowed down by BFA. Instead, in the presence of the AMI, BFLA, or MON CPV capsids were found in vesicles colocalizing with LAMP-2 to at least 20 h p.i. (Fig. 3C), while no colocalization was found with EEA1 in the presence of those drugs even though the drugs were added 30 min before inoculation of the virus and cells were fixed as late as 20 h p.i. (Fig. 3B). The result suggests that AMI, BFLA, and MON do not inhibit the trafficking of CPV from the early endosomes to the lysosomes. BFLA has been shown to inhibit trafficking from the early endosome to late endosome and to prevent fusion events between late endosomes and lysosomes (Clague et al., 1994; Van Weert et al., 1995). As CPV that earlier had been shown to colocalize with both recycling endosomal markers (Parker and Parrish, 2000; Suikkanen et al., 2002) and late endosomal/lysosomal marker LAMP-2 (Suikkanen et al., 2002), the recent results suggest that CPV does not need the route from early endosomes to late endosomes to enter to the lysosomes. Instead, our results suggest that CPV may enter the cells via early endosomes and perinuclear recycling route from which CPV is delivered to the lysosomal vesicles.

When the endocytic pathway was bypassed by microinjecting CPV into the cytoplasm of the cells, AMI inhibited the viral proliferation, but BFLA, MON, and BFA did not (not shown). This suggests that AMI inhibited some step(s) taking place after the endocytic phase in addition to its possible effect on the endocytic phase, while BFLA, MON, and BFA affected only the endocytic phase of CPV entry. Amiloride analogue 5-(*N*-ethyl-*N*-isopropyl)amiloride (EIPA) has been shown to inhibit the escape of adenovirus type 2 from endosomes without having any effect on viral uptake or on transferrin recycling (Meier et al., 2002). In the same study Meier et al. found that EIPA was also able to inhibit viral gene expression. This is in line with our findings that AMI was able to inhibit CPV infection even when added after CPV had already started its replication (Fig. 3A). To clarify the role of exposure of VP1 N-terminus in entry process, we infected cells with heat-treated CPV exposing VP1 N-termini in the presence of the drugs. Heat-treated CPV caused infection such as nontreated CPV in the absence of the drugs and infections of both heat-treated CPV and nontreated CPV were inhibited in the presence of the drugs (Figs. 3A and 5), indicating that the pH-induced exposure of N-terminal end of VP1 is not sufficient for the release of CPV from vesicles.

TfR is known to recycle back to the cell membrane in noninfected cells (Mayor et al., 1993). It has been shown

earlier by cytoplasmic microinjections of antibodies against the TfR cytoplasmic tail that CPV-TfR interaction persists for several hours. These microinjections inhibited CPV infection when carried out at 4 h p.i. (Parker et al., 2001). We found here that CPV capsids colocalize with TfR from the beginning of the entry to 10 h p.i. (Fig. 6A), indicating that the receptor is present while CPV is released to the cytoplasm. Furthermore, in CPV-infected cells more TfRs were found from lysosomal vesicles at 8 h p.i. than at 1 h p.i. (Fig. 6B). The result may indicate that the presence of CPV changed the routing of TfRs toward the lysosomes perhaps by clustering the receptors (Marsh et al., 1995). This result supports the idea presented above, that CPV enters the cells via recycling route but is later rerouted to the degradative pathway.

To be released to the cytoplasm, CPV must engage in some kind of interaction with the vesicle membrane. Aggregation of CPV to the lysosomal membrane was evident from LSM images (not shown) and immuno-EM (Fig. 4). Such an interaction was especially apparent in the presence of the BFLA, MON, and BFA (Fig. 4) that did not allow CPV to escape from the vesicles, and even in the presence of AMI, which seemed to allow some viruses to escape (Fig. 4). The frame showing lysosomes in the presence of BFA is especially interesting in that the label can be seen at a few spots concentrated on both sides of the lysosomal membrane (Fig. 4), possibly showing CPV in the process of penetration through the membrane. Unfortunately, at the present resolution of the electron micrographs, fine structure of the membrane is not seen.

Viral escape from endosomes has been investigated by cointernalization viruses or viral proteins with fluid-phase markers such a dextran, calcein, carboxyfluorescein, and horse radish peroxidase (HRP) (Prchla et al., 1995; Ruiz et al., 1994; Suomalainen et al., 1999). Evidence for two different mechanisms of escape used by adenoviruses or human rhinovirus type 2 (HRV2) has been found by cointernalization of differently sized dextrans with the viruses or virus proteins. Adenovirus was found to be able to release endosomal dextran almost size-independently, whereas release by HRV2 was shown to be highly size dependent (Prchla et al., 1995). Escape mechanism of CPV has been studied earlier by cointernalization of alpha-sarcin, where no disruption of endosomes was found (Parker and Parrish, 2000). In the present study we cointernalized small dextrans together with the virus to detect changes in membrane permeability. When rhodamine-labeled dextrans (M_r 3000 or M_r 10,000) were coendocytosed with CPV, the M_r 3000 dextran was able to penetrate to the cytoplasm and migrate further into the nucleus, while the M_r 10,000 dextran was not able to escape from endosomal membranes in the absence or presence of the CPV (Fig. 7). Control experiments showed that when endocytosed alone and chased for 20 h, both dextrans remained in endocytic vesicles and did not reach the nucleus (Fig. 7A). This indicates that CPV modified the permeability of the late-endosomal or lysosomal membrane, allowing the smaller dextran to leak out (Fig. 7B), suggesting that dextran release caused by CPV is highly size-dependent as shown earlier for HRV2 (Prchla et al., 1995). These observations are in line with the results of Parker et al., who showed that the endosomal membrane retained α-sarcin when coendocytosed with CPV (Parker and Parrish, 2000).

Time schedule of viral membrane permeabilization and the effect of the drugs (AMI, BFLA, BFA, or MON) on that was assayed by determining the percentage of cells showing released dextran in the cytosol and in the nucleus (Fig. 7C). CPV-induced release of the M_r 3000 dextran was observed at 8 h p.i. and later time points, while the viruses are being released to cytoplasm as shown in our earlier studies (Suikkanen et al., 2002). In the present study none of studied drugs was able to inhibit release of dextran despite the fact that they arrested CPV in the lysosomal structures. This suggests that membrane permeabilization, probably caused by viral PLA_2 activity, is not the only function needed for release of CPV from vesicles. VP3, a proteolytic cleavage product derived from VP2, contains conserved hydrophobic polyglysine region at N-terminus (Bloom et al., 1988; Chen et al., 1986 and reviewed in Cotmore and Tattersall, 1987) and this polyglysine region has been suggested to be inserted into the membrane (Cortes et al., 1993). At present, the role of VP3 is largely unknown and its role needs to be investigated. Furthermore, it seems unlikely that CPV, which is released to the cytoplasm in rather intact form (Vihinen-Ranta et al., 2002), would be able to penetrate through a pore of a size that would allow M_r 3000 dextran but not M_r 10 000 dextran to pass through the membrane. Thus, leakage may not necessarily indicate pore formation. An argument against pore formation would also be that a pore in the membrane would cause a rapid equilibration of the pH gradient across the membrane. As discussed above, there are reasons to believe that the maintaining of endosomal acidic pH may be an important factor in the penetration. Thus, the mechanism of the escape remains unsolved and warrants further investigation.

It is known that enveloped viruses use fusion with plasma membrane or with endosomal membranes to reach cytoplasm. Membrane interactions of nonenveloped viruses are less well understood. However, rhinovirus, poliovirus, and coxsackie virus are known to be able to interact with lipid bilayers. Furthermore, it has been shown that cell-surface nonsialyl glycolipids might also play a critical role as receptors for several viruses (Bhat et al., 1991; Brown et al., 1993). Recently, lipids have been shown to contribute to the organization and functions of the vacuolar system. Endosomes have been shown to have a mosaic of structural and functional membrane domains (Gruenberg, 2001). For example, CCVs are enriched in phosphatidylinositol 4- and 5-phosphates, which seem to have a key role of regulating CCVs (Jost et al., 1998). Phosphatidylinositol-3-phosphates which interact with proteins containing a FYVE or a PX domain seem to be concentrated to early endosomal membranes (Gillooly et al., 2000, 2001; Si-

monsen and Stenmark, 2001 and reviewed by Simonsen et al., 2001). Furthermore, lysophosphatidic acid and phosphatidylinositol-3,5-bisphosphate (PtdIns(3,5)P_2) are suggested to be characteristic for late endosomes (Kobayashi et al., 1998, 2002; Shisheva et al., 2001), while sphingolipids are abundant in recycling endosomes (Gagescu et al., 2000). In addition to sphingolipids, sulfatides have been found to colocalize with recycling endosomal markers such as Rab11 (Hölttä-Vuori et al., 2002). In present study we assayed CPV binding to sphingolipids and to phosphoinositides to investigate if CPV binds to lipids and if the binding differs between studied membrane lipids. Results showed that CPV was able to interact with several phosphoinositides including PtdIns(4,5)P_2 (generally found in CCVs), PtdIns(3)P (usually concentrated to early endosomal membranes), sulfatide (enriched in recycling endosomal membrane components), and PtdIns(3,5)P_2 and lysophosphatic acid found from late endosomal membranes, suggesting that CPV might be able to interact the membranes of these organelles also in vivo. Lipid binding seemed to be Ca^{2+}-dependent as 5 mM EDTA reduced CPV's ability to bind to studied lipids (excluding sulfatide). Surprisingly, heated capsids showing exposed VP1 N-terminae and VP1 antibody-treated capsids had equal ability to bind to lipids as nontreated capsids, suggesting that VP1 is not responsible for membrane binding. This further suggests that lipid binding and PLA_2 activity of CPV capsids are independent activities associated with the capsids. A possible role of these lipids as coreceptors needed for membrane penetration warrants further investigation.

Several arguments speak in favor of PLA_2 activity being involved in the entry, as follows: (1) the PLA_2 activity has been located in the N-terminal part of VP1, (2) this part was exposed at 3–8 h p.i. when CPV has reached lysosomes, (3) the lysosomal interior is known to be acidic, and (4) the PLA_2 activity was activated by incubation of CPV at an acidic pH. An interesting possibility is that the PLA_2 activity of CPV capsids is responsible for the observed modification of membrane permeability. (5) PLA_2 inhibitors inhibited CPV entry, indicating that PLA_2 activity is essential for the successful infection. The exposure of VP1 was not sufficient to allow CPV to penetrate to the cytoplasm in the presence of lysosomotropic drugs, suggesting that there might be some other factors (perhaps VP3 or receptor(s)) than PLA_2 activity that are needed for parvoviral membrane penetration process.

Materials and methods

Cells and virus

Norden Laboratories feline kidney (NLFK) cells were grown and maintained in Dulbecco's modified Eagle's medium (DMEM) supplemented with 10% fetal calf serum (Gibco, Paisley, UK). Canine parvovirus type 2 (CPV-d) was derived from a plasmid clone of virus, as previously described (Parker et al., 2001), and was grown in NLFK cells in 175-cm^2 cell-culture flasks (Nunc, Roskilde, Denmark) for 5 to 7 days and then stored at −20°C. Then, 300 ml of thawed culture medium was centrifuged at 3000*g* for 30 min and concentrated by ultrafiltration with 500-kDa filter (Amicon ultrafiltrator). Viruses were pelleted with ultracentrifugation at 173,000*g* for 2 h and resuspended in 900 μl of phosphate-buffered saline (pH 7.4) (PBS). The suspension was sonicated at low power and extracted with chloroform. Then full and empty capsids were separated from the aqueous phase of chloroform extraction by isopycnic centrifugation in 45% cesium chloride gradient; opalescent bands were collected with a syringe and capsids were pelleted by ultracentrifugation at 245,000*g* for 2 h. The pellets were resuspended in 100 μl PBS.

Assay of virus proliferation

To determine CPV proliferation, infected cells were incubated for 20 h, after which the number of fluorescent nuclei was determined with immunofluorescence microscopy. The primary antibody was MaCPV or MaNS1 (see below). Proliferation was quantified as the ratio of cells with fluorescent nuclei to the total number of cells, $n = 300$.

Antibodies

RaVP1 to synthetic peptide representing a part of the unique region of VP1 originated from the laboratory of prof. P. Tattersall and S. Cotmore (Yale University, New Haven, CT). This antibody has been shown not to react with VP2 and to react with CPV capsids only after the N-termimus VP1 has become exposed (Cotmore et al., 1997). Mouse monoclonal antibody to CPV (Mab8) (Strassheim et al., 1994; Wikoff et al., 1994) and to N-terminal unique sequence of VP1 (MaVP1) and to nonstructural protein-1 (MaNS1) as well as RaCPV were from Prof. Parrish (Comell University, Ithaca, NY). Monoclonal antibodies to EEA1 and to cation-indepenent mannose-6-phosphate receptor (Ci-MPR) were generous gifts from Varpu Marjomäki (Juuti-Uusitalo et al., 2000). Monoclonal antibody to LAMP-2 was from Developmental Studies Hybridoma Bank (University of Iowa, Iowa City, IA). Monoclonal antibodies to transferrin receptor were from Dako (Carpinteria, CA) and Molecular Probes. Alexa 546 and 488 conjugated goat anti-mouse and goat anti-rabbit antibodies were from Molecular Probes. Nanogold-conjugated anti-rabbit or anti-mouse IgG were from Nanoprobes (Yaphank, NY). Alkaline phosphatase conjugated swine anti-mouse antibody was from Dako.

Chemicals

Bafilomycin A_1, monensin, brefeldin A, quinacrine, AA-$COCF_3$, and amiloride (*N*-amidino-3,5-diamino-6-chloropyrazinecarboxamide) were from Sigma. Manoalide was

from BioMol (Hamburg, Germany). Dextrans (M_r 3000 or 10,000) labeled with rhodamine were purchased from Molecular Probes. All other chemicals were from Merck (Germany) and were of highest grade available.

Treatment of capsids with elevated temperature and with PLA_2 inhibitors

Purified heavy capsids of CPV (0.3–0.7 mg/ml in PBS) were incubated for 2 min on heat block thermostated at 37–75°C (±2°C), after which the samples were cooled gradually to room temperature. To introduce PLA_2 inhibitors to the heated capsids manifesting PLA_2 activity, capsids were incubated with manoalide (5–10 μM), quinacrine (0.02–2 mM), or $AACOCF_3$ (0.02–10 mM) for 1 h at room temperature with agitation. Unbound quinacrine was removed by pelleting CPV capsids by ultracentrifugation at 245,000 *g* for 2 h. The pellets were resuspended in original volume of PBS. Antibodies (2.5 mg/ml) to VP1-terminal end (RaVP1) or to VP2 (MaCPV) were incubated with purified and heated (2 min, 65°C) capsids (0.5 mg/ml) for 1 h in room temperature with agitation. Heat-treated capsids, capsids both heated and PLA_2-inhibitor treated, as well as capsids both heated antibody treated were used for PLA_2 activity assay.

Treatment of capsids with acidic buffers

Samples of CPV dissolved in 0.9% NaCl were diluted in 0.1 M citrate buffer pH 4.0, 5.0, 6.0, or 7.0 and incubated for 5 min at room temperature, and half of the samples was brought to neutrality by adding predetermined aliquots of 1 M Tris base. The other half of the samples was used immediately for PLA_2 activity assay without neutralization.

Assay of phospholipase A_2 activity

A commercial kit obtained from Cayman Chemical (MI, USA) was used to assay for phospholipase A_2 activity of CPV capsids in vitro according to the instructions provided by the manufacturer. The assay uses the 1,2-dithio analog of diheptanoyl phosphatidylcholine, which serves as a substrate for most PLA_2s (Hendrickson et al., 1983). Upon hydrolysis of the thioester bond at the sn-2 position by PLA_2, free thiols were detected by using DTNB (5,5′-dithio-bis-(2-nitrobenzoic acid)); 3–6 μg CPV capsids were used for these measurements. To control the effect of the low pH buffer on the assay system, we used buffer pH 4 as a sample. No unspecific signal caused by low pH was detected.

Immunofluorescence microscopy

For immunofluorescense studies 80% confluent cells grown on coverslips (diameter 13 mm) were inoculated with DNA containing particles of CPV (m.o.i. 40–50). To study the effects of endocytosis-modulating drugs, 0.4 mM AMI, 500 nM BFLA, 20 nM BFA, or 500 nM MON was added to the cells 30 min before inoculation of the virus and the drugs were maintained until fixation. After different times postinfection coverslips were rinsed with PBS and fixed with 4% paraformaldehyde (PFA) in PBS. After being incubated with permeabilization buffer (containing 1% bovine serum albumin (BSA), 1% Triton X-100, and 0.01% sodium azide in PBS) for 15 min, the coverslips were incubated with primary antibodies diluted with permeabilization buffer for 45 min at room temperature and rinsed several times with permeabilization buffer before incubation with secondary antibody (45 min at room temperature). Coverslips were finally rinsed several times with permeabilization buffer and embedded with mowiol-DABCO (30 mg/ml). Confocal microscopy was conducted on a Zeiss LSM 510 inverted microscope (equipped with Nomarski DIC).

Preembedding labeling for immunoelectron microscopy

Cells were grown on 35-mm plastic culture dishes to 80% confluency. The cells were incubated with CPV (m.o.i. 50) in DMEM for 20 h in the presence or absence of AMI, BFLA, BFA, or MON. Drugs were added on the top of the cells 30 min before virus and maintained until fixation. After 1–20 h dishes were washed with 0.1 M phosphate buffer, pH 7.4 and the cells were fixed with PLP for 2 h at RT (Brown and Farquhar, 1989). After rinsing with sodium phosphate buffer, cells were permeabilized for 8 min at RT with phosphate buffer containing 0.01% saponin and 0.1% BSA or with 0.05% Triton X-100 in 0.1 M phosphate buffer if the target was to visualize nuclear antigens. Primary antibody (MaCPV or RaVP1) and gold-conjugated secondary antibody were diluted in permeabilization buffer and incubated on the top of the cells for 1 h at RT. Between and after labelings, cells were washed with permeabilization buffer. Cells were postfixed with with 1% glutaraldehyde in 0.1 M phosphate buffer for 10 min at RT, quenched with 50 mM NH_4Cl in phosphate buffer, and washed with both phosphate buffer and water. Cells were treated in the dark with HQ-silver (Nanoprobes) for 2 min, followed by washes with water and gold toning solutions (2% sodium acetate 3 × 5 min, 0.05% gold chloride 10 min on ice, 0.3% sodium thiosulphate 2 × 10 min on ice). After washes with water, the cells were postfixed with 1% osmium tetroxide in 0.1 M phosphate buffer for 1 h at 4°C, dehydrated with a descending concentration series of ethanol, and stained with 2% uranyl acetate. Plastic capsules filled with Epon LX-112 (Ladd Research Industries, Williston, VT) were placed upside-down on top of the cells. After polymerization, the capsules were warmed up to 100°C and removed carefully, and horizontal sections were cut with an ultramicrotome (Ultracut 8008, Reichert-Jung) set to 50 nm, picked up on a grid, stained with 2% uranyl acetate and lead citrate, and viewed with an electron microscope JEM-1200EX (Jeol, Japan).

Microinjection of the CPV capsids

Capillary microinjection into NLFK cells was performed using the transjector 5246 and the micromanipulator 5171 (Eppendorf, Hamburg, Germany) connected to an inverted IMT-2 microscope (Olympus Optical Co., Tokyo, Japan). Needles were pulled from glass capillaries (diameter 1.2 mm, Clark Electromedical Instruments, Reading, UK) using a P-97 needle puller (Sutter Instruments, Novato, CA). For the microinjection experiments, cells were grown to 80% confluency on microgrid size coverslips (175-nm grid size; Eppendorf). Cells were injected into cytoplasm with 0.1 to 0.5 pl of viral capsids at 0.5 to 1 mg/ml in PBS. For details of drug treatments, immunolabeling, and imaging (please see Immunofluorescence microscopy).

Release of dextran particles from endosomal vesicles

Cells were grown on coverslips (diameter 13 mm) to 80% confluency. The cells were pulsed with rhodamine-conjugated lysine-fixable dextran (M_r 3000 or 10,000, 3 mg/ml) and H-CPV for 15 min in the presence or absence of 0.4 mM AMI, 500 nM BFLA, 20 nM BFA, or 500 nM MON, after which they were chased for 2, 8, or 16 h in the presence or absence of 0.4 mM AMI, 500 nM BFLA, 20 nM BFA, or 500 nM MON. Controls were made without the virus. Cells were fixed with 4% PFA and imaging was made with Leitz DM RBE fluorescence microscope (Leica, Wetzlar, Germany) equipped with Spot CCD camera and Spot RT software (Diagnostic Instruments Inc., Sterling Heights, MI). Percentage of cells showing cytoplasmic and/or nuclear fluorescence was calculated (approximately 1500 cells/sample). The presence of the CPV was tested every time by indirect immunofluorescence labeling as described above. Immunofluorescence labeling of the viral capsids was carried out as described above. In addition, anti-LAMP-2 antibody was used to show late endosomal/lysosomal localization of the dextrans and viruses.

Assay of binding of CPV to lipids

To study lipid binding of CPV capsids, we used lipid-containing membranes (PIP-strips and sphingo-strips) purchased from Molecular Probes. Membranes were first blocked overnight at 4°C with 3% fatty acid free bovine serum albumin in Tris-buffered saline (TBS, pH 7.4). Then membranes were incubated two times o/n at 4°C in TBS–Tween (0.1%) containing 3% fatty acid free BSA and 1 μg/ml purified CPV capsids. The membranes were then washed with TBS–Tween several times. Bound viruses were detected using capsid antibody (MaCPV) and alkaline phosphatase conjugated secondary antibody, after which substrate was introduced for 5 min and reaction was stopped.

Acknowledgments

We thank Professor Colin Parrish for providing antibodies. We also thank Katja Sääjärvi, Pirjo Kauppinen, Einari Niskanen, Paavo Niutanen, and Raimo Pesonen for providing excellent technical assistance, and Eija Jokitalo for guidance with nanogold labeling. The work was supported by grants from the Academy of Finland (Contract 10210), the National Technology Agency (TEKES, Contract 70026/00), and Galilacus Oy.

References

Agbandje, M., Mckenna, R., Rossmann, M.G., Strassheim, M.L., Parrish, C.R., 1993. Structure determination of feline panleukopenia virus empty particles. Proteins 16 (2), 155–171.

Bartlett, J.S., Wilcher, R., Samulski, R.J., 2000. Infectious entry pathway of adeno-associated virus and adeno-associated virus vectors. J. Virol. 74 (6), 2777–2785.

Basak, S., Turner, H., 1992. Infectious entry pathway for canine parvovirus. Virology 186, 368–376.

Bhat, S., Spitalnik, S.L., Gonzalez-Scarano, F., Silberberg, D.H., 1991. Galactosyl ceramide or a derivative is an essential component of the neural receptor for human immunodeficiency virus type 1 envelope glycoprotein gp120. Proc. Natl. Acad. Sci. USA 88 (16), 7131–7134.

Bloom, M.E., Alexandersen, S., Perryman, S., Lechner, D., Wolfinbarger, J.B., 1988. Nucleotide sequence and genomic organization of Aleutian mink disease parvovirus (ADV): sequence comparisons between a nonpathogenic and a pathogenic strain of ADV. J. Virol. 62 (8), 2903–2915.

Brown, K.E., Anderrsson, S.M., Young, N.S., 1993. Erythrocyte P antigen: cellular receptor for B19 parvovirus. Science 262, 114–117.

Brown, W.J., Farquhar, M.G., 1989. Immunoperoxidase methods for the localization of antigens in cultured cells and tissue sections by electron microscopy. Methods Cell Biol. 31 (553), 553–569.

Chardonnet, Y., Dales, S., 1970. Early events in the interaction of adenoviruses with HeLa cells. II. Comparative observations on the penetration of types 1, 5, 7, and 12. Virology 40 (3), 478–485.

Chen, K.C., Shull, B.C., Moses, E.A., Lederman, M., Stout, E.R., Bates, R.C., 1986. Complete nucleotide sequence and genome organization of bovine parvovirus. J. Virol. 60 (3), 1085–1097.

Clague, M.J., Urbé, S., Anieto, F., Gruenberg, J., 1994. Vacuolar ATPase activity is required for endosomal carrier vesicle formation. J. Biol. Chem. 269, 21–24 (Vacuolar ATPase ECV).

Cortes, E., San Martin, C., Langeveld, J., Meloen, R., Dalsgaard, K., Vela, C., Casal, I., 1993. Topographical analysis of canine parvovirus virions and recombinant VP2 capsids. J. Gen. Virol. 74 (Pt. 9), 2005–2010.

Cotmore, S.E., Tattersall, P., 1987. The autonomously replicating parvoviruses of vertebrates. Adv. Virus Res. 33, 91–169.

Cotmore, S.F., D'abramo Jr., A.M., Ticknor, C.M., Tattersall, P., 1999. Controlled conformational transitions in the MVM virion expose the VP1 N-terminus and viral genome without particle disassembly. Virology 254 (1), 169–181.

Cotmore, S.F., D'abramo Jr., A.M., Carbonell, L.F., Bratton, J., Tattersall, P., 1997. The NS2 polypeptide of parvorirus MVM is required for capsid assembly in murine cells. Virology 231, 267–280.

D'arrigo, A., Bucci, C., Toh, B.H., Stenmark, H., 1997. Microtubules are involved in bafilomycin A1-induced tubulation and Rab5-dependent vacuolation of early endosomes. Eur. J. Cell. Biol. 72 (2), 95–103.

Dales, S., Chardonnet, Y., 1973. Early events in the interaction of adenovirus with HeLa cells. Virology 56, 465–483.

De Sena, J., Mandel, B., 1977. Studies on the in vitro uncoating of poliovirus. II. Characteristics of the membrane-modified particle. Virology 78 (2), 554–566.

Dorsch, S., Liebisch, G., Kaufmann, B., Von Landenberg, P., Hoffmann, J.H., Drobnik, W., Modrow, S., 2002. The VP1 unique region of parvovirus B19 and its constituent phospholipase A2-like activity. J. Virol. 76 (4), 2014–2018.

Douar, A.M., Poulard, K., Stockholm, D., Danos, O., 2001. Intracellular trafficking of adeno-associated virus vectors: routing to the late endosomal compartment and proteasome degradation. J. Virol. 75 (4), 1824–1833.

Fricks, C.E., Hogle, J.M., 1990. Cell-induced conformational change in poliovirus: externalization of the amino terminus of VP1 is responsible for liposome binding. J. Virol. 64 (5), 1934–1945.

Gagescu, R., Demaurex, N., Parton, R.G., Hunziker, W., Huber, L.A., Gruenberg, J., 2000. The recycling endosome of Madin–Darby canine kidney cells is a mildly acidic compartment rich in raft components. Mol. Biol. Cell. 11 (8), 2775–2791.

Gillooly, D.J., Morrow, I.C., Lindsay, M., Gould, R., Bryant, N.J., Gaullier, J.M., Parton, R.G., Stenmark, H., 2000. Localization of phosphatidylinositol 3-phosphate in yeast and mammalian cells. EMBO J. 19 (17), 4577–4588.

Gillooly, D.J., Simonsen, A., Stenmark, H., 2001. Cellular functions of phosphatidylinositol 3-phosphate and FYVE domain proteins. Biochem. J. 355 (Pt. 2), 249–258.

Giranda, V.L., Heinz, B.A., Oliveira, M.A., Minor, I., Kim, K.H., Kolatkar, P.R., Rossmann, M.G., Rueckert, R.R., 1992. Acid-induced structural changes in human rhinovirus 14: possible role in uncoating. Proc. Natl. Acad. Sci. USA 89, 10213–10217.

Girod, A., Wobus, C.E., Zadori, Z., Ried, M., Leike, K., Tijssen, P., Kleinschmidt, J.A., Hallek, M., 2002. The VP1 capsid protein of adeno-associated virus type 2 is carrying a phospholipase A2 domain required for virus infectivity. J. Gen. Virol. 83 (Pt. 5), 973–978.

Gomez Yafal, A., Kaplan, G., Racaniello, V.R., Hogle, J.M., 1993. Characterization of poliovirus conformational alteration mediated by soluble cell receptors. Virology 197 (1), 501–505.

Greve, J.M., Forte, C.P., Marlor, C.W., Meyer, A.M., Hoover-Litty, H., Wunderlich, D., Mcclelland, A., 1991. Mechanisms of receptor-mediated rhinovirus neutralization defined by two soluble forms of ICAM-1. J. Virol. 65 (11), 6015–6023.

Gruenberg, J., 2001. The endocytic pathway: a mosaic of domains. Nat. Rev. Mol. Cell. Biol. 2 (10), 721–730.

Harada, M., Shakado, S., Sakisaka, S., Tamaki, S., Ohishi, M., Sasatomi, K., Koga, H., Sata, M., Tanikawa, K., 1997. Bafilomycin A1, a specific inhibitor of V-type H+-ATPases, inhibits the acidification of endocytic structures and inhibits horseradish peroxidase uptake in isolated rat sinusoidal endothelial cells. Liver 17 (5), 244–250.

Hendrickson, H.S., Hendrickson, E.K., Dybvig, R.H., 1983. Chiral synthesis of a dithiolester analog of phosphatidylcholine as a substrate for the assay of phospholipase A2. J. Lipid Res. 24 (11), 1532–1537.

Hölttä-Vuori, M., Tanhuanpää, K., Mobius, W., Somerharju, P., Ikonen, E., 2002. Modulation of cellular cholesterol transport and homeostasis by Rab11. Mol. Biol. Cell. 13 (9), 3107–3122.

Hoover-Litty, H., Greve, J.M., 1993. Formation of rhinovirus-soluble ICAM-1 complexes and conformational changes in the virion. J. Virol. 67 (1), 390–397.

Johnson, L.S., Dunn, K.W., Pytowski, B., Mcgraw, T.E., 1993. Endosome acidification and receptor trafficking: bafilomycin A1 slows receptor externalization by a mechanism involving the receptor's internalization motif. Mol. Biol. Cell 4, 1251–1266.

Jost, M., Simpson, F., Kavran, J.M., Lemmon, M.A., Schmid, S.L., 1998. Phosphatidylinositol-4,5-bisphosphate is required for endocytic coated vesicle formation. Curr. Biol. 8 (25), 1399–1402.

Juuti-Uusitalo, K., Airenne, K.J., Laukkanen, A., Punnonen, E.L., Olkkonen, V.M., Gruenberg, J., Kulomaa, M., Marjomaki, V., 2000. Selective targeting of avidin/mannose 6-phosphate receptor chimeras to early or late endosomes. Eur. J. Cell. Biol. 79 (7), 458–468.

Kaplan, G., Peters, D., Racaniello, V.R., 1990. Poliovirus mutants resistant to neutralization with soluble cell receptors. Science 250 (4987), 1596–1599.

Kim, S., Ikeuchi, K., Groopman, J., Baltimore, D., 1990. Factors affecting cellular tropism of human immunodeficiency virus. J. Virol. 64 (11), 5600–5604.

Kobayashi, T., Beuchat, M.H., Chevallier, J., Makino, A., Mayran, N., Escola, J.M., Lebrand, C., Cosson, P., Gruenberg, J., 2002. Separation and characterization of late endosomal membrane domains. J. Biol. Chem. 277 (35), 32157–32164.

Kobayashi, T., Stang, E., Fang, K.S., De Moerloose, P., Parton, R.G., Gruenberg, J., 1998. A lipid associated with the antiphospholipid syndrome regulates endosome structure and function. Nature 392 (6672), 193–197.

Li, Y., Zadori, Z., Bando, H., Dubuc, R., Fediere, G., Szelei, J., Tijssen, P., 2001. Genome organization of the densovirus from Bombyx mori (BmDNV-1) and enzyme activity of its capsid. J. Gen. Virol. 82 (Pt. 11), 2821–2825.

Lippincott-Schwartz, J., Yuan, L., Tipper, C., Amherdt, M., Orci, L., Klausner, R.D., 1991. Brefeldin A's effects on endosomes, lysosomes, and the TGN suggest a general mechnism for regulating organelle structure and membrane traffic. Cell 67, 601–616.

Marsh, E.W., Leopold, P.L., Jones, N.L., Maxfield, F.R., 1995. Oligomerized transferrin receptors are selectively retained by a lumenal sorting signal in a long-lived endocytic recycling compartment. J. Cell. Biol. 129 (6), 1509–1522.

Marsh, M., Helenius, A., 1989. Virus entry into animal cells. in: Maramorosch, K., Murphy, F.A., Shatkin, A.J. (Eds.), Advances in Virus Research, Vol. 36. Academic Press, London, pp. 107–151.

Mayor, S., Presley, J.F., Maxfield, F.R., 1993. Sorting of membrane components from endosomes and subsequent recycling to the cell surface occurs by a bulk flow process. J. Cell Biol. 121, 1257–1269.

Meier, O., Boucke, K., Hammer, S.V., Keller, S., Stidwill, R.P., Hemmi, S., Greber, U.F., 2002. Adenovirus triggers macropinocytosis and endosomal leakage together with its clathrin-mediated uptake. J. Cell Biol. 158 (6), 1119–1131.

Miyazawa, N., Crystal, R.G., Leopold, P.L., 2001. Adenovirus serotype 7 retention in a late endosomal compartment prior to cytosol escape is modulated by fiber protein. J. Virol. 75 (3), 1387–1400.

Noel, J., Pouyssegur, J., 1995. Hormonal regulation, pharmacology, and membrane sorting of vertebrate Na+/H+ exchanger isoforms. Am. J. Physiol. 268 (2 Pt. 1), C283–C296.

Ogier, G., Chardonnet, Y., Doerfler, W., 1977. The fate of type 7 adenovirions in lysosomes of HeLa cells. Virology 77 (1), 66–77.

Paradiso, P.R., 1981. Infectious process of the parvovirus H-1: correlation of protein content, particle density, and viral infectivity. J. Virol. 39 (3), 800–807.

Paradiso, P.R., Rhode 3rd., S.L., Singer, Ii., 1982. Canine parvovirus: a biochemical and ultrastructural characterization. J. Gen. Virol. 62 (Pt 1), 113–125.

Parker, J.S., Murphy, W.J., Wang, D., O'brien, S.J., Parrish, C.R., 2001. Canine and feline parvoviruses can use human or feline transferrin receptors to bind, enter, and infect cells. J. Virol. 75 (8), 3896–3902.

Parker, J.S., Parrish, C.R., 2000. Cellular uptake and infection by canine parvovirus involves rapid dynamin-regulated clathrin-mediated endocytosis, followed by slower intracellular trafficking. J. Virol. 74 (4), 1919–1930.

Prchla, E., Plank, C., Wagner, E., Blaas, D., Fuchs, R., 1995. Virus-mediated release of endosomal content in vitro: different behavior of adenovirus and rhinovirus serotype 2. J. Cell Biol. 131 (1), 111–123.

Pressman, B.C., 1976. Biological applications of ionophores. Annu. Rev. Biochem. 45, 501–530.

Ros, C., Burckhardt, C.J., Kempf, C., 2002. Cytoplasmic trafficking of minute virus of mice: low-pH requirement, routing to late endosomes, and proteasome interaction. J. Virol. 76 (24), 12634–12645.

Ruiz, M.C., Alonso-Torre, S.R., Charpilienne, A., Vasseur, M., Michelangeli, F., Cohen, J., Alvarado, F., 1994. Rotavirus interaction with isolated membrane vesicles. J. Virol. 68 (6), 4009–4016.

Seth, P., Fitzgerald, D.J., Willingham, M.C., Pastan, I., 1984a. Role of a low-pH environment in adenovirus enhancement of the toxicity of a Pseudomonas exotoxin-epidermal growth factor conjugate. J. Virol. 51 (3), 650–655.

Seth, P., Willingham, M.C., Pastan, I., 1984b. Adenovirus-dependent release of 51Cr from KB cells at an acidic pH. J. Biol. Chem. 259 (23), 14350–14353.

Seth, P., Willingham, M.C., Pastan, I., 1985. Binding of adenovirus and its external proteins to Triton X-114. Dependence on pH. J. Biol. Chem. 260 (27), 14431–14434.

Shisheva, A., Rusin, B., Ikonomov, O.C., Demarco, C., Sbrissa, D., 2001. Localization and insulin-regulated relocation of phosphoinositide 5-kinase PIKfyve in 3T3-L1 adipocytes. J. Biol. Chem. 276 (15), 11859–11869.

Simonsen, A., Stenmark, H., 2001. PX domains: attracted by phosphoinositides. Nat. Cell. Biol. 3 (8), E179–E182.

Simonsen, A., Wurmser, A.E., Emr, S.D., Stenmark, H., 2001. The role of phosphoinositides in membrane transport. Curr. Opin. Cell Biol. 13 (4), 485–492.

Stein, B.S., Sussman, H.H., 1986. Demonstration of two distinct transferrin receptor recycling pathways and transferrin-independent receptor internalization in K562 cell. J. Biol. Chem. 261, 10319–10331.

Strassheim, M.L., Gruenberg, A., Veijalainen, P., Sgro, J.-Y., Parrish, C.R., 1994. Two dominant neutralizing antigenic determinants of canine parvovirus are found on the threefold spike of the virus capsid. Virology 198, 175–184.

Suikkanen, S., Sääjärvi, K., Hirsimäki, J., Välilehto, O., Reunanen, H., Vihinen-Ranta, M., Vuento, M., 2002. Role of recycling endosomes and lysosomes in dynein-dependent entry of canine parvovirus. J. Virol. 76 (9), 4401–4411.

Suomalainen, M., Nakano, M.Y., Keller, S., Boucke, K., Stidwill, R.P., Greber, U.F., 1999. Microtubule-dependent plus- and minus end-directed motilities are competing processes for nuclear targeting of adenovirus. J. Cell. Biol. 144 (4), 657–672.

Tattersall, P., Cotmore, S.F., 1988. The nature of parvoviruses, in: Pattison, J.R. (Ed.), Parvoviruses and Human Disease. CRC Press, Boca Raton, FL, pp. 5–41.

Tattersall, P., Shatkin, A.J., Ward, D.C., 1977. Sequence homology between the structural polypeptides of minute virus of mice. J. Mol. Biol. 111 (4), 375–394.

Tosteson, M.T., Chow, M., 1997. Characterization of the ion channels formed by poliovirus in planar lipid membranes. J. Virol. 71 (1), 507–511.

Tsao, J., Chapman, S., Agbandje, M., Keller, W., Smith, K., Wu, H., Luo, M., Smith, T.J., Rossman, M.G., Compans, R.W., Parrish, C.R., 1991. The three-dimensional structure of canine parvovirus and its functional implications. Science 251, 1456–1464.

Tullis, G.E., Burger, L.R., Pintel, D.J., 1992. The trypsin-sensitive RVER domain in the capsid proteins of minute virus of mice is required for efficient cell binding and viral infection but not for proteolytic processing in vivo. Virology 191 (2), 846–857.

Tullis, G.E., Burger, L.R., Pintel, D.J., 1993. The minor capsid protein VP1 of autonomous parvovirus minute virus of mice is dispensable for encapsidation of progeny sinle-stranded DNA but is required for infectivity. J. Virol. 67, 131–141.

Van Weert, A.W., Dunn, K.W., Gueze, H.J., Maxfield, F.R., Stoorvogel, W., 1995. Transport from late endosomes to lysosomes, but not sorting of integral membrane proteins in endosomes, depends on the vacuolar proton pump. J Cell Biol 130 (4), 821–834.

Vihinen-Ranta, M., Kakkola, L., Kalela, A., Vilja, P., Vuento, M., 1997. Characterization of a nuclear localization signal of canine parvovirus capsid proteins. Eur. J. Biochem. 1, 389–394.

Vihinen-Ranta, M., Kalela, A., Mäkinen, P., Kakkola, L., Marjomäki, V., Vuento, M., 1998. Intracellular route of canine parvovirus entry. J. Virol. 72, 802–806.

Vihinen-Ranta, M., Wang, D., Weichert, W.S., Parrish, C.R., 2002. The VP1 N-terminal sequence of canine parvovirus affects nuclear transport of capsids and efficient cell infection. J. Virol. 76 (4), 1884–1891.

Vihinen-Ranta, M., Yuan, W., Parrish, C.R., 2000. Cytoplasmic trafficking of the canine parvovirus capsid and its role in infection and nuclear transport. J. Virol. 74 (10), 4853–4859.

Weichert, W.S., Parker, J.S.L., Wahid, A.T.M., Chang, S.-F., Meier, E., Parrish, C.R., 1998. Assaying for structural variation in the parvovirus capsid and its role in infection. Virology 250, 106–117.

Wickham, T.J., Filardo, E.J., Cheresh, D.A., Nemerow, G.R., 1994. Integrin alpha v beta 5 selectively promotes adenovirus mediated cell membrane permeabilization. J. Cell Biol. 127 (1), 257–264.

Wikoff, W.R., Wang, G., Parrish, C.R., Cheng, R.H., Strassheim, M.L., Baker, T.S., Rossmann, M.G., 1994. The structure of a neutralized virus: canine parvovirus complexed with neutralizing antibody fragment. Structure 2 (7), 595–607.

Xie, Q., Chapman, M.S., 1996. Canine parvovirus capsid structure, analyzed at 2.9 A resolution. J. Mol. Biol. 264 (3), 497–520.

Yun, C.H., Tse, C.M., Nath, S.K., Levine, S.A., Brant, S.R., Donowitz, M., 1995. Mammalian Na+/H+ exchanger gene family: structure and function studies. Am. J. Physiol. 269 (1 Pt. 1), G1–G11.

Zádori, Z., Szelei, J., Lacoste, M.-C., Li, Y., Gariépy, S., Raymond, P., Allaire, M., Nabi, I.R., Tijssen, P., 2001. A viral phospholipase A_2 is required for parvovirus infectivity. Dev. Cell 1, 291–302.